PROCEEDINGS OF SPIE

SPIEDigitalLibrary.org/conference-proceedings-of-spie

Multi-tone modulated continuous-wave lidar

Rasul Torun, Mustafa M. Bayer, Imam Uz Zaman, Ozdal Boyraz

Rasul Torun, Mustafa M. Bayer, Imam Uz Zaman, Ozdal Boyraz, "Multi-tone modulated continuous-wave lidar," Proc. SPIE 10925, Photonic Instrumentation Engineering VI, 109250V (4 March 2019); doi: 10.1117/12.2507565

SPIE.

Event: SPIE OPTO, 2019, San Francisco, California, United States

Multi-tone Modulated Continuous Wave Lidar

Rasul Torun[a], Mustafa M. Bayer[a], Imam Uz Zaman[a], and Ozdal Boyraz[a]

[a]Department of Electrical Engineering and Computer Science, University of California, Irvine, Irvine, CA, USA, 92697

ABSTRACT

Because of its high range and resolution, light detection and ranging (LIDAR) is a significant technology for numerous applications, such as autonomous vehicles, robotics, aerial or terrestrial mapping, and atmospheric research. Current lidar market is mainly occupied by conventional pulsed time of flight lidars. However, recently emerging companies are utilizing frequency modulated continuous wave lidars for improved and robust range resolution, dynamic range, sensitivity and simultaneous velocity measurement. Here, we propose and demonstrate multi-tone modulated continuous wave (MTCW) lidar system made of a CW laser with multiple fixed RF tones for a high precision range finding and velocimetry. In the proposed approach, the interference of the scattered light with the reference is detected by a PIN photodiode to extract the modulation information. Since, the acquired light is traveled all the way to the target and back to the beam splitter, it carries the range and velocity information about the target as phase and frequency shift, respectively, on the RF modulation tones. We use 1550nm light source and multiple RF tone modulations ranging from 50 MHz to 6 GHz to demonstrate proof of principle for range finding. We also provide sine fitting algorithms on the measured RF tones to extract the range and velocity information in a single shot RF measurement. We show that the precision and range information are scaled by the selection of RF tones. By an engineered selection of RF tones and a laser source, the measurement precision can be increased without compromising the range.

Keywords: Lidar, range finding, velocimetry, RF modulation, multi-tone modulation, heterodyne detection, interference, sine fitting

1. INTRODUCTION

Over the past years, light detection and ranging (lidar) technology has been vastly used in military applications[1] and atmospheric sciences.[2] The wide range of lidar applications include detection of remote objects, measurement of the distances and ranges,[3] creation of topographical images,[4] detection of aerosol particles,[5,6] and investigation of ozone layers.[7,8] With the rise of interest in self-driving cars and unmanned aerial vehicles (UAV), lidar systems have grabbed a recent attention for proximity sensing and collision prevention.[9–14] However, majority of these current research activities aim to achieve more robust, accurate and sensitive measurements in longer ranges via improvement of the receiver architectures,[15] and utilizing the signal processing technologies.[16,17] Most of the lidar based ranging systems rely on the pulsed time of flight (PToF) methodology, which is the exploitation of the time delay between transmission and reception of the incident and backscattered laser pulses, respectively. To further increase the timing accuracy in such systems, it is required to operate with short pulses and to have high temporal resolution, thus it is necessary to use fast electronics. To minimize the timing errors, estimation methods can be facilitated by capturing several measurements of the same target. Moreover, PToF lidar lacks the ability of velocity detection and direction information of propagating targets.[18]

Nowadays, there are a few recent lidar applications that utilize the continuous wave (CW) lasers as in amplitude modulated continuous wave (AMCW), and frequency modulated continuous wave (FMCW) lidars.[19–21] AMCW lidar systems modulate the intensity of the light, while keeping the laser frequency constant. In such

Further author information: (Send correspondence to R.T. or O.B.)
R.T.: E-mail: rtorun@uci.edu
M.M.B.: E-mail: bayerm@uci.edu
I.Z.: E-mail: zamani@uci.edu
O.B.: E-mail: oboyraz@uci.edu

Photonic Instrumentation Engineering VI, edited by Yakov G. Soskind,
Proc. of SPIE Vol. 10925, 109250V · © 2019 SPIE · CCC
code: 0277-786X/19/$18 · doi: 10.1117/12.2507565

architectures, high-speed radio frequency (RF) electronics are required to modulate the transmitted CW laser intensity through electro-optic modulators. In AMCW lidars, the speed of the modulation depicts the accuracy of the ranging. On the receiver side, the high-speed RF requirement can be mitigated by demodulation or implementing super heterodyne receivers that convert the high-frequency-tones to base band signals. One way to acquire the range information with AMCW is via the convolution of the local oscillator with the time-delayed backscattered signal as in phase shift lidars.[18] The other method is by electronic heterodyne detection to generate a beat note proportional to the target distance as in linearly chirped lidars.[19] By employing AMCW lidars and implementing precision improvement techniques such as multiple signal classification and harmonic distortion cancellation, <5mm precision was previously reported for ranges less than 12m.[22–24]

On the other hand, FMCW lidars operate by facilitating frequency sweeping of the light sources such as frequency tunable lasers or frequency modulated CW lasers with a chirped RF signal. The collected signal is detected via optical heterodyning by using a slow square-law detector, while the slower electronics can record the generated beating frequency.[18] Since the range of the same target is measured with several frequencies, the acquired results are more robust and accurate compared to the other lidar architectures.[19] In addition, FMCW lidars have the potential of detecting the speed and direction information of a given target simultaneously.[25,26] For the short ranges (<10m), it is possible to achieve sub-mm resolutions with a FMCW system that exploits wide-band frequency tuning with a sweeping source.[27–29] But for the medium ranges (∼100m), the resolution reduces to ∼5cm with a bandwidth that is limited to 5GHz.[30] In practice, the sweeping frequency can be increased up to a few GHz due to the stability of the laser source, which further limits the range resolution to cm level.[31,32] On the other hand, for wide band (200nm) frequency swept lasers, slow (kHz) sweep rate becomes the limiting factor. Very recently, frequency combs are implemented to achieve more than a THz bandwidth that corresponds to μm resolutions in a short range.[33]

In this work, a new multi-tone modulated continuous wave lidar technology that has the ability to provide high precision range and velocity information of static and moving targets is presented. In the proposed approach, CW lasers are simultaneously modulated with carefully selected RF tones. At the receiver end, the interference of the scattered light with the reference arm is detected by a photodiode, thus yielding a heterodyne detection. Since, the acquired light is traveled all the way to the target and back to the beam splitter, the received signal carries the range and velocity information of the target as phase and frequency shift on the detected RF tones, respectively. After interfering the received signal with the reference, phase shift will convert to amplitude variation. Therefore, we exploited the relative amplitude variations of RF tones to extract the range information. The proposed MTCW lidar architecture is investigated theoretically and verified with numerical simulations. In addition, a proof of concept experiment has been performed to show the range measurements of static targets. By facilitating 2.5GHz and 6GHz RF tones, short range measurements with accuracy of 1cm are demonstrated. It is possible to further improve the accuracy of the proposed MTCW lidar by increasing the tone frequencies, data extrapolation and signal processing algorithms. Moreover, the recent developments in highly coherent narrow linewidth laser technologies can also provide the required dynamics for over kilometer distances, which will enhance the MTCW lidar architecture. In overall, the proposed system is a suitable candidate to be used in aerial or satellite based remote sensing that demands cm level accuracy for long distances.

2. METHODOLOGY

Figure 1 shows the schematic of the multi-tone continuous wave lidar system. The system is driven by a CW laser source that is amplitude modulated by a Lithium Niobate ($LiNbO_3$) Mach Zehnder modulator (MZM) to create well separated optical tones. After collimation and beam expansion, signal is split into two via a free-space beam splitter (BS) cube as reference and measurement. The measurement signal is incident on the target. The reflected beam is then collected back at the same transmit aperture. After collecting the reflected signal, it is sent to an interferometer that enables the superposition of the transmit signal and the reference signal before a detector. The photodetector is used to detect interference signal and capture RF tones needed for the range finding. Due to the difference in phase accumulation at different optical tones at a given target distance, we will have nonuniform amplitudes across the RF frequencies. By carefully evaluating the strength of tone powers, we can estimate the path length that the optical beam takes from source to the target and back to the detector. In this study, we have developed an algorithm that recognizes the amplitude nonuniformity

across the tone frequencies and precisely detect the range information from these amplitude variations. If there is a moving target, the system can also detect the Doppler shift to identify the velocity and direction in the same simple configuration. The number of the RF tones and their frequencies are selected carefully for desired range of distances, and the precision of interest. Consequently, the proposed method is facilitating multi-tone RF modulation, optical heterodyning and sine fitting algorithms that enable acquisition of range and velocity information in a single shot measurement by eliminating the need of frequency, amplitude or phase sweeping.

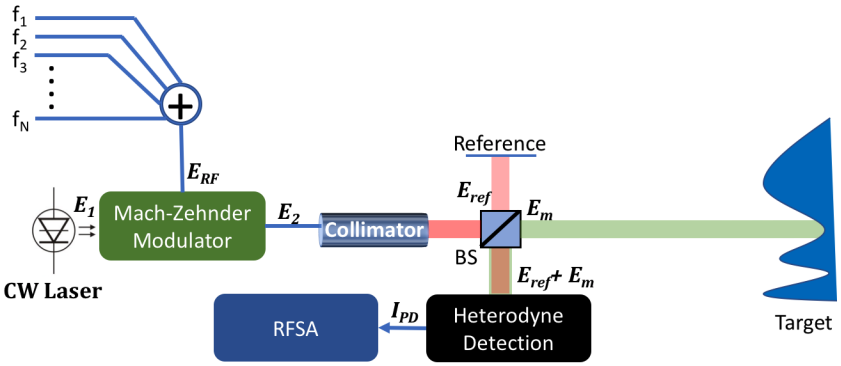

Figure 1. Schematic of the proposed multi-tone continuous wave lidar system. BS: Beam Splitter, RFSA: RF Spectrum Analyzer

2.1 Analytical Model

The unmodulated complex optical field at the output of CW laser can be modeled as[34]

$$E_1 = A_0 exp(j\omega_0 t + j\phi_0) \tag{1}$$

where A_0 is the amplitude of the light's electric field, ω_0 is the angular frequency of optical carrier, and ϕ_0 is the phase of initial light beam. Later, this optical carrier is intensity modulated by a waveform that is sum of sinusoidal signals,

$$E_{RF} = \sum_{i=1}^{N} A_i cos(2\pi f_i t + \phi_i) \tag{2}$$

where A_i, f_i, and ϕ_i are the amplitude, frequency and phase of i^{th} RF tone respectively. Mach Zehnder modulator is biased at quadrature bias ($V_{DC} = \frac{V_\pi}{2}$) and driven with balanced RF signals (E_{RF}) under push-pull configuration. Therefore, its field transfer function ($cos(0.5\pi v_m/V_\pi)$) will convert to $T_{MZM} = \frac{1}{\sqrt{2}} - \frac{\pi}{2\sqrt{2}V_\pi} E_{RF}$ for low modulation depth ($m = \pi A_i/V_\pi \ll 1$) after trigonometric conversions and small angle approximations. Low modulation depth is facilitated to operate MZM in linear regime and suppress higher order distortion tones.

The modulated field will be $E_2 = T_{MZM} \times E_1$, therefore

$$E_2 = \frac{A_0}{\sqrt{2}} exp(j\omega_0 t + j\phi_0) - \frac{mA_0}{4\sqrt{2}} \sum_{i=1}^{N} exp(j(\omega_0 + 2\pi f_i)t + j(\phi_0 + \phi_i)) + exp(j(\omega_0 - 2\pi f_i)t + j(\phi_0 - \phi_i)) \tag{3}$$

where RF tone amplitudes are selected equal, hence modulation depth, m, is same for all RF tones. Later, modulated light is transferred to free space through a collimator and split into two via a beam splitter. While one of the signals is travelling to the target (measurement signal), the other is kept inside the system to be used

as a local oscillator (reference signal) in coherent detection. Both signals accumulate phase during propagation and the returned signals at the input of the detector can be represented as

$$E_{ref,m} = \frac{A_0}{2\sqrt{2}}\alpha_{ref,m}exp(j\omega_0 t + j\phi_0 + j\omega_0\frac{2L_{ref,m}}{c}) \\ -m\frac{A_0}{4\sqrt{2}}\alpha_{ref,m}\sum_{i=1}^{N}[exp(j(\omega_0+2\pi f_i)t + j(\phi_0+\phi_i) + j(\omega_0+2\pi f_i)\frac{2L_{ref,m}}{c}) \\ +exp(j(\omega_0-2\pi f_i)t + j(\phi_0-\phi_i) + j(\omega_0-2\pi f_i)\frac{2L_{ref,m}}{c})] \quad (4)$$

where L_{ref} and L_m are the distances between the beam splitter and reference mirror and target, and α_{ref} and α_m are the linear loss coefficients while traveling such distances respectively. At the detector, the reference and measurement signals will be mixed and the current output of the PIN photodiode will be $I_{PD} = RP_{in} = R(E_{ref}+E_m)(E_{ref}+E_m)^*$ where R is the responsivity of the detector and P_{in} is input optical power to the detector. The phase shift of each tone will convert to amplitude variations at different RF tones that is described as

$$I_{PD} = I_{PD,ave} - \frac{1}{4}RmA_0^2\sum_{i=1}^{N}(\alpha_{ref}\alpha_m+\alpha_{ref}^2)cos(2\pi f_i t+\frac{4\pi}{c}L_{ref}f_i) - (\alpha_{ref}\alpha_m+\alpha_m^2)cos(2\pi f_i t+\frac{4\pi}{c}L_m f_i) \quad (5)$$

where $I_{PD,ave}$ is the average photodiode current that is the sum of all beating terms between identical frequency components in reference and measurement signals including optical carrier and RF tones. As seen in Eq. (5), when the reference and measurement signals interfere constructively for a tone frequency, f_i, second term gives the minimum value $(\alpha_{ref}^2 - \alpha_m^2)$, therefore photodiode current will be maximum. It will be the opposite for the destructive interference case.

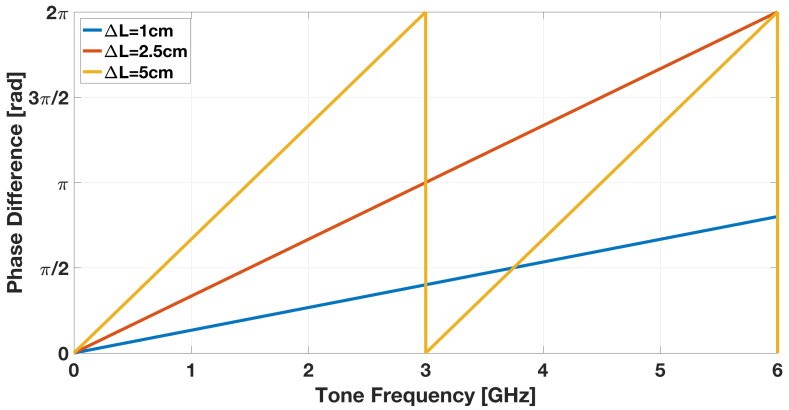

Figure 2. Variation of phase difference between reference and measurement signals with respect to tone frequencies within 6GHz bandwidth for ΔL=1cm, 2.5cm, and 5cm.

As is clear in Eq. (5), each RF frequency tone, f_i, accumulates different phase while light is traveling towards the target. The phase difference between reference and measurement arms is $\Delta\phi_i = \frac{4\pi}{c}\Delta L f_i$, hence proportional to path length difference (ΔL) and RF modulation tones (f_i) as demonstrated in Fig. 2. Here, blue curve shows the unit phase variation per cm distance over the bandwidth of 6GHz. Therefore, when ΔL increases, slope of the line also increases. After total phase difference exceeds 2π, periodic triangular signal will occur due to wrapping.

The phase difference between backscattered light and the reference will produce a variation in amplitudes for different tones after interference. After recording the power of each tone, the data points are fit into a sinusoidal

signal to extract the frequencies of interest, where total constructive and destructive interference occur. The frequency difference between two consecutive peaks will determine the range information according to Eq. (6) below.

$$\frac{4\pi}{c}\Delta L(f_{p2} - f_{p1}) = 2\pi \Rightarrow \Delta L = \frac{c}{2\Delta f} \tag{6}$$

In MTCW lidar, we are specifically interested in the sinusoidal fit over the measured tone powers as shown in Fig. 3. After investigating constructive and destructive interference cases in Eq. (5), the amplitude of such fitting will be $A_{fit} = \frac{1}{4}RmA_0^2[\alpha_m(\alpha_{ref} + \alpha_m)]$, and modulation depth of the oscillation will be $m_{osc} = \frac{\alpha_m}{\alpha_{ref}}$. Since the backscattered power from the target is so low, the reference arm should be attenuated to preserve extinction ratio and modulation depth of oscillation. However, RF heterodyne detection can be pursued in electrical domain to further enhance the signal-to-noise ratio (SNR) of the detection system.

2.2 Numerical verification

We modeled the full system of the proposed MTCW lidar in the computer environment that includes the modulator and detector nonlinearities, laser and detector noises, and losses in the measurement arm by using Mathematica and Matlab to verify the experimental results.

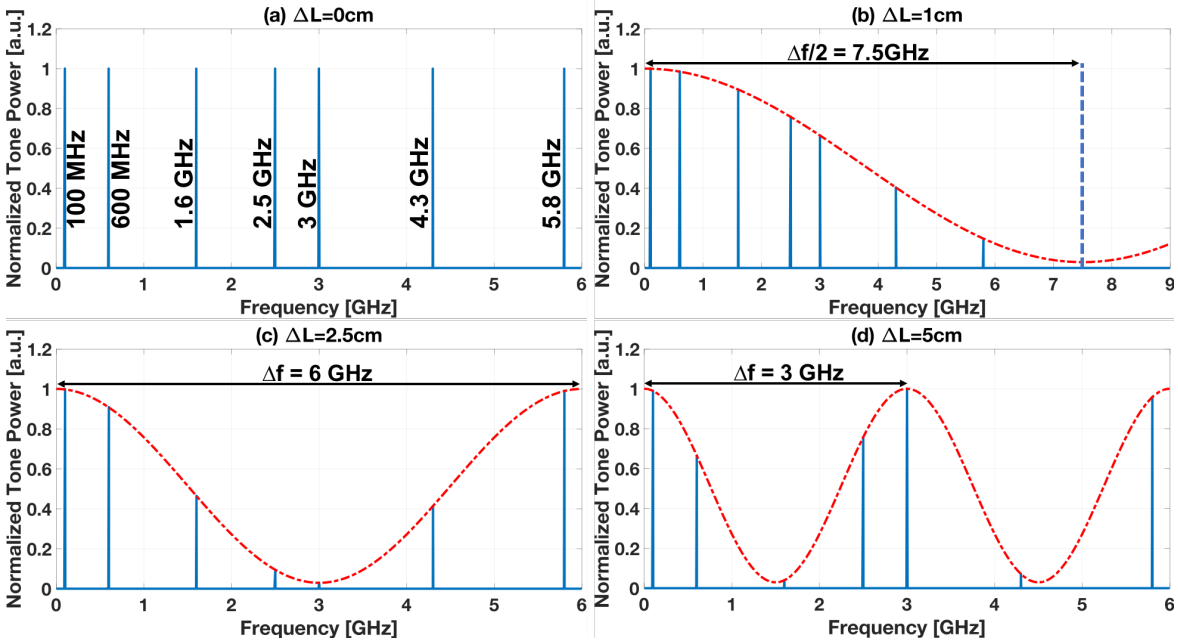

Figure 3. RF tone power variation for various target distances where (a) $\Delta L = 0$ that does not generate any amplitude variation and (b-d) ΔL= 1, 2.5 and 5 cm that generate 15GHz, 6GHz and 3GHz separation between consecutive peaks

In Fig. 3, the evolution of the tone powers is demonstrated while the range of the target is moved up to 5cm from its initial position. The modulation depth is set to 5% and only 3dB additional loss is inserted to measurement arm, hence ($\alpha_{ref} = 1, \alpha_m = \sqrt{0.5}$). In order to eliminate overlapping of actual tones with higher order distortions such as harmonic distortions ($2f, 3f, ...$) and intermodulation distortion ($2f_2 \pm f_1, 2f_1 \pm f_2, ...$), we selected RF tones as 100MHz, 600MHz, 1.6GHz, 2.5GHz, 3GHz, 4.3GHz and 5.8GHz with the same amplitudes as shown in Fig. 3(a). When the target is 5cm away, the light propagates a total distance of 10cm back and forth from the target that creates peaks at every 3GHz. Therefore, while 3GHz tone have same amplitude as before, 1.6GHz is degraded the most due to the close proximity to the valley point at 1.5GHz that experience the complete destructive interference at the detector (Fig. 3(d)). When the target distance is halved as in

Fig. 3(c), the period of sinusoidal fitting increases to 6GHz as expected from Eq. (6). Therefore, to achieve high resolutions, large bandwidth is required. For example, by facilitating 50GHz RF bandwidth, the system can achieve 3mm resolution. Such higher resolutions can also be achieved by extrapolating the data of lower frequency tones and signal processing without going to X-band modulation. An example to extrapolation is demonstrated in Fig. 3(b) where a sinusoidal fit that requires 15GHz bandwidth to observe at least one full cycle can be extracted from the tones inside 6GHz actual bandwidth. It is also important to note that the period of sinusoidal fit in Fig. 3 is same as the period of triangle function in Fig. 2 for the same path length differences.

When the target range increases, the consecutive peaks of sinusoidal fit come closer to each other due to inverse proportionality of range and frequency. However, the same modulation pattern repeats itself according to the period of greatest common divisor (GCD) of all RF tones. For the given tones GCD is 100MHz, therefore the same modulation pattern is repeating itself in every 1.5 meters. This MTCW system is designed for the fine range measurements at the last portion of true range information (L_{act}) that can be represented as $L_{act} = N \times L_{rep} + L_f$ where L_{rep} is the distance of modulation pattern repetition and L_f is the final range information that can be extracted from this system. However, it is not possible to extract the number of repetitions (N) directly. Using quasi-CW signals can eliminate the uncertainty by providing coarse range measurement results similar to PToF lidars.

3. EXPERIMENTAL VERIFICATION

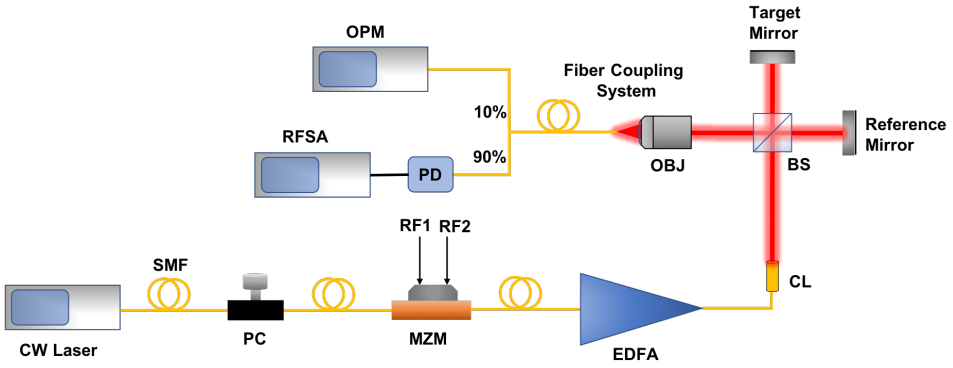

Figure 4. Full experimental setup

In order to demonstrate system performance, the proposed lidar system is established on the optical table as shown in Fig. 4. We used a CW laser operating at 1550nm with 14mW average power. The laser output is sent to an 8GHz Lithium Niobate ($LiNbO_3$) Mach-Zehnder intensity modulator to modulate light with the sum of two RF tones. Two RF tones generated by Agilent RF Signal Generators are combined by a coaxial 2-way power combiner and fed into modulators RF port. Modulators quadrature bias operation is ensured by a DC power supply. Modulated light is first amplified by an Erbium doped fiber amplifier (EDFA) with >10dB gain and transferred to the free space via a collimator with 2.1mm beam waist and 0.95mrad beam divergence. The transmitted beam then split into two branches through a non-polarizing 50-50 beam splitter (BS) cube. In this experiment, for demonstration purposes, we used Aluminum mirrors with >95% reflectivity as a target and reference, hence $\alpha_{ref} \approx \alpha_m \approx 1$. The target mirror is moved on an optical rail for coarse measurements and a micrometer stage is used for fine tuning. Back reflected lights from the mirrors are recombined with the same beam splitter and directed to the heterodyne detection mechanism. As a detector, we used >12.5GHz, fiber coupled InGaAs PIN photodiode (PD). Therefore, we established a free space to fiber coupling system by using 3D micrometer stages and 10X objective lens with a numerical aperture of 0.25. The coupling efficiency of the system is greater than 25%. After coupling to the fiber, through a 90/10 power splitter, average power is observed in an optical power meter (OPM), while spectral measurements are facilitated with an RF Spectrum Analyzer (RFSA). The acquired spectra are recorded and further post-processed in Matlab to extract range information via sinusoidal fitting algorithms.

For proof of concept demonstration, we modulate the CW laser by using two RF tones at 2.5GHz and 6GHz, and the measurement arm is moved slowly to observe interference. Figure 5(a) shows that 2.5GHz and 6GHz tones are forming waveforms with 6cm and 2.5cm periods, respectively. The results are in a perfect correlation with the theoretical expectations. Figure 5(b) indicates the amount of error in the system at each measurement distance for individual tones. The rms error of the system is calculated from the error graph as 0.0972 and 0.0905 for 2.5GHz and 6GHz tones, respectively.

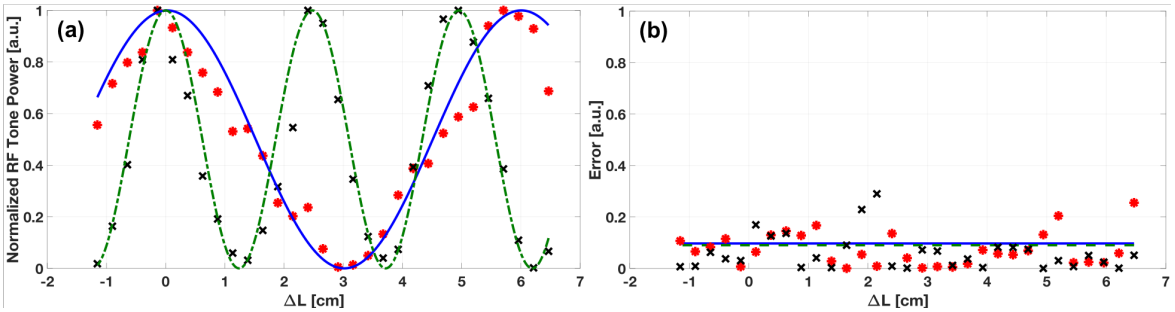

Figure 5. (a) Multi-tone measurement by using two tones at 2.5GHz and 6GHz (b) Calculated error between experimental data and theoretical expectation for individual tones at 2.5GHz (dots) and 6GHz (crosses) in multi-tone measurement system. Rms error values at 2.5GHz and 6GHz are represented as solid and dashed lines respectively.

4. CONCLUSION

In this work, we demonstrated multi-tone modulated continuous wave lidar system. The system has the capability of providing the high precision range and velocity information of static and moving targets. Here, we demonstrated proof of concept experiments along with theoretical and numerical analysis for range measurements in static environments. Further applications of the proposed method for scattering or moving targets can be implemented by engineering the source power, receiver sensitivity and utilizing the Doppler frequency shift.

ACKNOWLEDGMENTS

This work is supported by National Aeronautics and Space Administration Cooperative Agreement Partnerships with Universities (NNX16AT64A) and Office of Naval Research (N00014-18-1-2845).

REFERENCES

[1] Stann, B. L., Ruff, W. C., and Sztankay, Z. G., "Intensity-modulated diode laser radar using frequency-modulation/continuous-wave ranging techniques," **35**(11), 3270–3279.

[2] Ansmann, A., Wandinger, U., Riebesell, M., Weitkamp, C., and Michaelis, W., "Independent measurement of extinction and backscatter profiles in cirrus clouds by using a combined raman elastic-backscatter lidar," **31**(33), 7113–7131.

[3] Braun, A., Chien, C. Y., Coe, S., and Mourou, G., "Long range, high resolution laser radar," **105**(1), 63–66.

[4] Bufton, J. L., Garvin, J. B., Cavanaugh, J. F., Ramos-Izquierdo, L. A., Clem, T. D., and Krabill, W. B., "Airborne lidar for profiling of surface topography," **30**(1), 72–79.

[5] Ansmann, A. and Mller, D., "Lidar and atmospheric aerosol particles," in [*Lidar: Range-Resolved Optical Remote Sensing of the Atmosphere*], Weitkamp, C., ed., *Springer Series in Optical Sciences*, 105–141, Springer New York.

[6] Mamouri, R.-E. and Ansmann, A., "Potential of polarization/raman lidar to separate fine dust, coarse dust, maritime, and anthropogenic aerosol profiles," **10**(9), 3403–3427. WOS:000411128000001.

[7] Sullivan, P. P., Moeng, C.-H., Stevens, B., Lenschow, D. H., and Mayor, S. D., "Structure of the entrainment zone capping the convective atmospheric boundary layer," **55**(19), 3042–3064.

[8] Quan, J., Gao, Y., Zhang, Q., Tie, X., Cao, J., Han, S., Meng, J., Chen, P., and Zhao, D., "Evolution of planetary boundary layer under different weather conditions, and its impact on aerosol concentrations," **11**(1), 34–40.

[9] Luettel, T., Himmelsbach, M., and Wuensche, H., "Autonomous ground vehiclesconcepts and a path to the future," **100**, 1831–1839.

[10] Himmelsbach, M., Mller, A., Luettel, T., and Wuensche, H. J., "LIDAR-based 3d object perception," in [*Proceedings of 1st International Workshop on Cognition for Technical Systems*],

[11] Ramasamy, S., Sabatini, R., Gardi, A., and Liu, J., "LIDAR obstacle warning and avoidance system for unmanned aerial vehicle sense-and-avoid," **55**, 344–358.

[12] Kidono, K., Miyasaka, T., Watanabe, A., Naito, T., and Miura, J., "Pedestrian recognition using high-definition LIDAR," in [*2011 IEEE Intelligent Vehicles Symposium (IV)*], 405–410.

[13] Aufrere, R., Gowdy, J., Mertz, C., Thorpe, C., Wang, C. C., and Yata, T., "Perception for collision avoidance and autonomous driving," **13**(10), 1149–1161. WOS:000185418800008.

[14] Shinzato, P. Y., Wolf, D. F., and Stiller, C., "Road terrain detection: Avoiding common obstacle detection assumptions using sensor fusion," in [*2014 IEEE Intelligent Vehicles Symposium Proceedings*], 687–692.

[15] Chen, Z., Fan, R., Li, X., Dong, Z., Zhou, Z., Ye, G., and Chen, D., "Accuracy improvement of imaging lidar based on time-correlated single-photon counting using three laser beams," **429**, 175–179.

[16] Godbaz, J. P., Cree, M. J., Dorrington, A. A., and Payne, A. D., "A fast maximum likelihood method for improving AMCW lidar precision using waveform shape," in [*2009 IEEE SENSORS*], 735–738.

[17] Godbaz, J. P., Cree, M. J., and Dorrington, A. A., "Understanding and ameliorating non-linear phase and amplitude responses in AMCW lidar," **4**(1), 21–42.

[18] Lum, D. J., Knarr, S. H., and Howell, J. C., "Frequency-modulated continuous-wave LiDAR compressive depth-mapping," **26**(12), 15420.

[19] Behroozpour, B., Sandborn, P. A. M., Wu, M. C., and Boser, B. E., "Lidar system architectures and circuits," **55**(10), 135–142.

[20] Amann, M.-C., Bosch, T. M., Lescure, M., Myllylae, R. A., and Rioux, M., "Laser ranging: a critical review of unusual techniques for distance measurement," **40**(1), 10–20.

[21] McManamon, P., [*Field Guide to Lidar*], SPIE.

[22] Whyte, R., Streeter, L., Cree, M. J., and Dorrington, A. A., "Application of lidar techniques to time-of-flight range imaging," **54**(33), 9654–9664.

[23] Payne, A. D., Dorrington, A. A., Cree, M. J., and Carnegie, D. A., "Improved measurement linearity and precision for AMCW time-of-flight range imaging cameras," **49**(23), 4392–4403.

[24] Dorrington, A. A., Cree, M. J., Payne, A. D., Conroy, R. M., and Carnegie, D. A., "Achieving sub-millimetre precision with a solid-state full-field heterodyning range imaging camera," **18**(9), 2809.

[25] Yoshikawa, E. and Ushio, T., "Wind ranging and velocimetry with low peak power and long-duration modulated laser," **25**(8), 8845–8859.

[26] Feneyrou, P., Leviandier, L., Minet, J., Pillet, G., Martin, A., Dolfi, D., Schlotterbeck, J.-P., Rondeau, P., Lacondemine, X., Rieu, A., and Midavaine, T., "Frequency-modulated multifunction lidar for anemometry, range finding, and velocimetry - 1. theory and signal processing," **56**(35), 9663–9675.

[27] Hariyama, T., Sandborn, P. A. M., Watanabe, M., and Wu, M. C., "High-accuracy range-sensing system based on FMCW using low-cost VCSEL," **26**(7), 9285–9297.

[28] Sandborn, P., Kaneda, N., Chen, Y.-K., and Wu, M. C., "Dual-sideband linear FMCW lidar with homodyne detection for application in 3d imaging," in [*Conference on Lasers and Electro-Optics (2016), paper STu4H.8*], STu4H.8, Optical Society of America.

[29] Sandborn, P. A. M., Hariyama, T., and Wu, M.-C., "Resolution-enhancement for wide-range non-linear FMCW lidar using quasi-synchronous resampling," in [*Imaging and Applied Optics 2017 (3D, AIO, COSI, IS, MATH, pcAOP) (2017), paper DW3F.3*], DW3F.3, Optical Society of America.

[30] Kim, T., Bhargava, P., and Stojanovic, V., "Optimal spectral estimation and system trade-off in long-distance frequency-modulated continuous-wave lidar," in [*2018 IEEE International Conference on Acoustics, Speech and Signal Processing (ICASSP)*], 1583–1587.

[31] Bosq, T. W. D. and Preece, B. L., "Frequency modulated continuous wave lidar performance model for target detection," in [*Infrared Imaging Systems: Design, Analysis, Modeling, and Testing XXVIII*], **10178**, 101780T, International Society for Optics and Photonics.

[32] Batet, O., Dios, F., Comeron, A., and Agishev, R., "Intensity-modulated linear-frequency-modulated continuous-wave lidar for distributed media: fundamentals of technique," **49**(17), 3369–3379.

[33] Trocha, P., Karpov, M., Ganin, D., Pfeiffer, M. H. P., Kordts, A., Wolf, S., Krockenberger, J., Marin-Palomo, P., Weimann, C., Randel, S., Freude, W., Kippenberg, T. J., and Koos, C., "Ultrafast optical ranging using microresonator soliton frequency combs," **359**(6378), 887–891.

[34] Mandel, L., "Complex representation of optical fields in coherence theory*," **57**(5), 613–617.